



Ammonia oxidation in $\text{Ba}_{0.5}\text{Sr}_{0.5}\text{Co}_{0.8}\text{Fe}_{0.2}\text{O}_{3-\delta}$ membrane reactor

Shumin Sun^{a,b}, M. Rebeilleau-Dassonneville^a, Xuefeng Zhu^a, Wenling Chu^{a,*}, Weishen Yang^{a,*}

^a State Key Laboratory of Catalysis, Dalian Institute of Chemical Physics, Chinese Academy of Sciences, Dalian 116023, China

^b Graduate School of the Chinese Academy of Sciences, Beijing 10039, China

ARTICLE INFO

Article history:

Available online 18 April 2009

Keywords:

Membrane reactor
Ammonia oxidation
Perovskite
 $\text{Ba}_{0.5}\text{Sr}_{0.5}\text{Co}_{0.8}\text{Fe}_{0.2}\text{O}_{3-\delta}$
Structural stability

ABSTRACT

Selective oxidation of ammonia to NO was studied in a dense mixed ion electron conducting $\text{Ba}_{0.5}\text{Sr}_{0.5}\text{Co}_{0.8}\text{Fe}_{0.2}\text{O}_{3-\delta}$ membrane reactor, which integrates the separation and catalytic reaction process in a single reactive separation unit. The influence of the temperature and feed concentration on the membrane reaction performance were investigated in detail. Under reaction conditions, the oxygen permeation flux through the dense membrane increases with increasing temperature and ammonia flow rate. The lower temperature and ammonia concentration can favor the formation of NO, in which higher catalytic performance is obtained, suggesting that the membrane reactor operation is much beneficial for selective oxidation of ammonia.

© 2009 Elsevier B.V. All rights reserved.

1. Introduction

Nitric acid is one of the most important bulk chemicals to produce fertilizer, detonator and dye. In industry, the production of nitric acid traditionally rely on platinum–rhodium alloy gauzes (5–10% Rh) as catalysts for the high-temperature ammonia oxidation reaction [1,2]. The oxidation of ammonia on noble metal gauzes mainly produce NO (94–96% yield) with N_2 and N_2O as by-products. From an engineering point of view, this reaction is well optimized [3], but this technology has some significant drawbacks, including high production cost and metal loss in the form of volatile oxides. Moreover, the nitric acid production is the largest source for N_2O emission in the chemical industry, and development of efficient and economical system for N_2O abatement is being required. These environmental and economic forces stimulate researchers to develop new catalysts replacing noble metals and new routes for ammonia oxidation reaction.

In the recent decades, a vast number of patents and papers claimed that less expensive oxides, such as Co_3O_4 , $\alpha\text{-Fe}_2\text{O}_3$ and Cr_2O_3 , showed promising performance in ammonia oxidation reaction [4,5]. However, the emission of N_2O is still unavoidable in the reaction. Accordingly, the design of novel routes for ammonia oxidation is strongly promoted in order to eliminate the N_2O production.

A novel process for ammonia oxidation using lanthanum ferrite-based perovskite membrane reactor was successfully

achieved by Perez-Ramirez et al., in which the high NO selectivity was obtained and no N_2O was formed [6,7]. Therefore, the exploitation of perovskite membrane reactor in ammonia oxidation affords a new path for the formation of NO due to high efficiency and minimal environmental pollution. Particularly, the membrane reactor integrates the separation and reaction process in a single reactive separation unit. As depicted in Fig. 1, on the feed side, gaseous O_2 in air was dissociated into O^{2-} in the surface of membrane, then O^{2-} diffuses toward the reaction side driven by the oxygen partial pressure gradient across the membrane. On the reaction side, NH_3 is oxidized by oxygen species which diffuse from the air side.

Our group has developed an excellent perovskite membrane based on $\text{Ba}_{0.5}\text{Sr}_{0.5}\text{Co}_{0.8}\text{Fe}_{0.2}\text{O}_{3-\delta}$ (BSCFO) by partially substituting Sr in $\text{SrCo}_{0.8}\text{Fe}_{0.2}\text{O}_{3-\delta}$ with Ba [8]. It was found that the BSCFO membrane possesses good phase stability and significant excellent oxygen permeability. Many selective oxidations have been carried out on the BSCFO membrane reactors [9–13] while no process for ammonia oxidation using BSCF membrane was attempted.

In this study, the oxidation of ammonia to nitric acid was firstly explored in a $\text{Ba}_{0.5}\text{Sr}_{0.5}\text{Co}_{0.8}\text{Fe}_{0.2}\text{O}_{3-\delta}$ membrane reactor. The reaction performance of the membrane reactor was investigated as functions of temperature, ammonia concentration. In addition, the effects of the reaction on the membrane surface were investigated.

2. Experimental

$\text{Ba}_{0.5}\text{Sr}_{0.5}\text{Co}_{0.8}\text{Fe}_{0.2}\text{O}_{3-\delta}$ oxide powder was synthesized by a combined citrate and EDTA complexation method. In this method, stoichiometric amounts of $\text{Ba}(\text{NO}_3)_2$, $\text{Fe}(\text{NO}_3)_3$, $\text{Sr}(\text{NO}_3)_2$ and

* Corresponding authors. Tel.: +86 411 84379073; fax: +86 411 84694447.
E-mail addresses: cwl@dicp.ac.cn (W. Chu), yangws@dicp.ac.cn (W. Yang).
URL: <http://www.yanggroup.dicp.ac.cn>

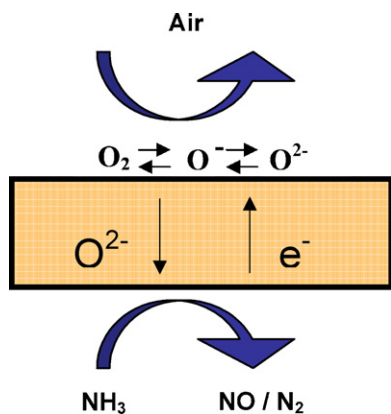


Fig. 1. Schematic of ammonia oxidation in perovskite membrane reactor.

$\text{Co}(\text{NO}_3)_2$ were fully dissolved in the mixture solution of NH_3 and EDTA. Under heating and stirring the citric acid (CA) was introduced with a molar ratio of Metal: EDTA:CA = 1:1.5:2. The obtained purple solution was heated at 90°C until a gel was formed. The gel was heated at 500°C for 30 min and then the obtained foam was calcined at 950°C for 3 h to get the mixed perovskite oxide. The as-synthesized powder was pressed into disks in a stainless steel module (17 mm in diameter) under a hydraulic pressure of 1.5 MPa. These green disks were then sintered in a SiC muffle oven under 1150°C for 5 h with a heating and cooling rate of 1 and $2^\circ\text{C}/\text{min}$, respectively.

The ammonia oxidation was studied using a reactor shown in Fig. 2. Membrane discs (1.4 mm thick) were sealed in between two quartz tubes (OD 18 mm, ID 15 mm) using gold rings as chemically inert sealant. The sealing was carried out at the beginning of experimental runs by heating at 1040°C for 10 h. The reactions were carried out in the temperature range of 800 – 1000°C by feeding air to the feed side and mixtures of NH_3 and He to the reaction side of the membrane. One membrane disc was just used for one temperature point. The oxygen permeation measurement was performed before the reaction. The inlet ammonia flow was varied in the range of 1.5 – 5 ml min^{-1} NH_3 with constant total flow rates of 130 ml min^{-1} controlled by mass flow controllers. The products (O_2 , N_2 , NO , N_2O and H_2O) were analyzed by an on-line Agilent 6890 connected to the HP Chemstation for data collection and analysis. A molecular sieve 13X column was used to separate O_2 , N_2 and NO and a Porapak Q column was used to separate N_2O

from the other gases. Ammonia concentrations in the feed and the product were determined by a conventional titration method. Firstly, the mixture of gases containing ammonia pass by a bottle with excess 0.1 mol l^{-1} sulfuric acid solution for 5 min to absorb ammonia, then a 0.1 mol l^{-1} NaOH solution was used to titrate the excess acid solution to get the concentration of ammonia in the feed or product gases. The nitrogen balance was within 10%. Gas leakage due to a bad sealing could be detected by monitoring nitrogen concentration in the permeation side during the oxygen permeation measurements. The leaked oxygen was less than 1% of the total detected oxygen. It is reasonable to assume the leaking of nitrogen and oxygen through pores is in accordance with the Knudsen diffusion mechanism, so the fluxes of leaked N_2 and O_2 have the following relationship:

$$J_{\text{N}_2}^{\text{leak}} : J_{\text{O}_2}^{\text{leak}} = \sqrt{32/28} \times \frac{0.79}{0.21}$$

For oxygen permeation measurement, the leakage of the system was calculated using the equation as follows:

$$\text{The leakage} = C_{\text{N}_2} \times \frac{0.21}{0.79} \times \frac{\sqrt{28/32}}{C_{\text{O}_2}} \times 100\%$$

where C_{O_2} , C_{N_2} are the measured oxygen concentrations of oxygen and nitrogen in the exited gas of the permeation side, respectively. The oxygen flux going through the membrane during the ammonia oxidation was calculated from the concentrations of all the products and the un-reacted oxygen in the tail gas.

The phase structure of perovskite oxide was determined by X-ray diffraction (XRD) using a Rigaku D/Max-2500 diffractometer (Cu $\text{K}\alpha$ radiation, operating at 40 kV and 250 mA) in the range of 20 – 80° with a scanning rate of 5°min^{-1} . The surface microstructure of fresh and used membrane disc was studied with a scanning electron microscopy (SEM, Quanta 200 FEG, FEI Company, operating at 20 kV). The element analysis of the membrane disc surface and cross-section was evaluated by SEM-EDX.

3. Results and discussion

3.1. Effect of temperature on membrane reaction

Fig. 3 shows the effect of the reaction temperature on the ammonia oxidation reaction at the ammonia flow rate of 1.5 ml min^{-1} , corresponding to a feed concentration of 1.1 vol.% NH_3 in the mixture of He and NH_3 . The total flow of ammonia and He was kept constant at 130 ml/min and the flow of air in the feed

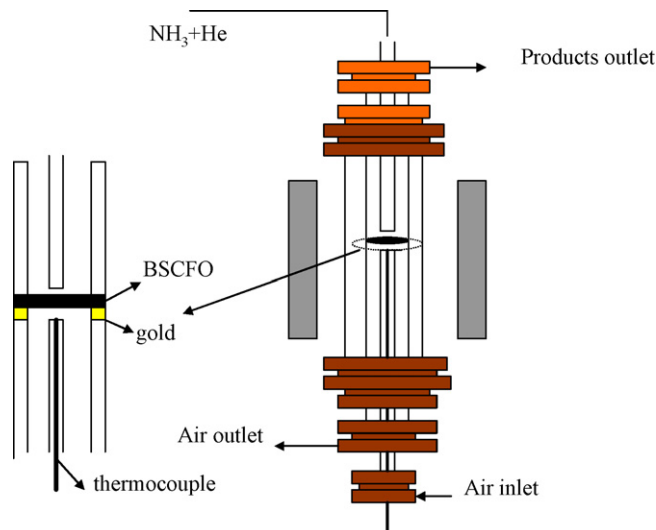


Fig. 2. Quartz reactor used in the membrane reaction.

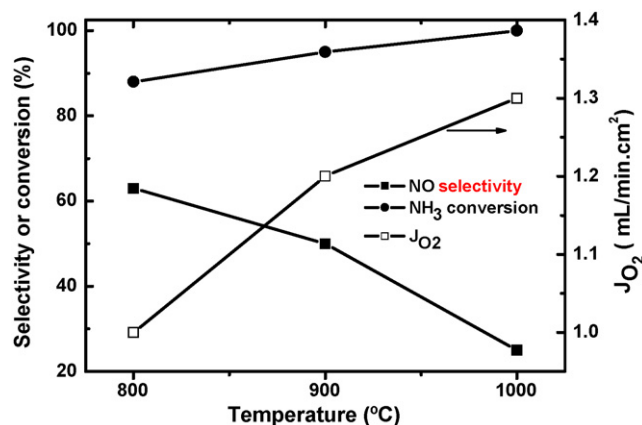


Fig. 3. Effect of temperatures on performance of membrane reactor. Ammonia flow rate is 1.5 ml/min and the total flow rate of ammonia and He is 130 ml/min , air flow rate is 50 ml/min . Thickness of the membrane: 1.4 mm.

side was 50 ml/min. As expected, during the experiments, the undesirable N_2O was not detected and N_2 was the only N-containing by-product with the perovskite membrane reactor, which confirmed the results reported by Perez-Ramirez et al. [6,7]. It is obvious from Fig. 3 that the oxygen permeation flux and ammonia conversion increased with increasing the temperature. From 800 to 1000 °C, the oxygen flux increased from 1.0 to 1.3 ml/min cm^2 , which was mainly attributed to the increase in oxygen diffusion and the surface exchange kinetics with the increasing reaction temperature. Meanwhile, it was observed that the ammonia conversion was increased from 84% to 100% with increasing the temperature from 800 to 1000 °C. On the contrary, NO selectivity decreased with increasing the reaction temperature. It is well known that the selectivity is associated with the surface oxygen bonding strength of the oxides [14–17]. For a given oxide catalyst, there is an optimal temperature for ammonia oxidation to obtain the highest NO selectivity. For example, an increase of the temperature for the maximum NO selectivity goes from Co_3O_4 (650 °C) to $\alpha-Fe_2O_3$ (750 °C) to $\alpha-Cr_2O_3$ (850 °C), which correlates with the increasing oxygen bonding strength of the oxides [17]. O_2 -TPD measurement claimed that a majority of oxygen of $Ba_{0.5}Sr_{0.5}Co_{0.8}Fe_{0.2}O_{3-\delta}$ desorbs around 400 °C, suggesting that for the $Ba_{0.5}Sr_{0.5}Co_{0.8}Fe_{0.2}O_{3-\delta}$ catalyst, the lower temperature could favor the route yielding NO due to its weak oxygen bonding strength as shown by the results.

3.2. Effect of feed concentration on the membrane reaction

Fig. 4 shows the effect of the concentration of ammonia in the feed on the ammonia oxidation reaction at the temperature of 800 °C. The total flow of NH_3 and He was 130 ml/min, different ammonia concentrations were achieved by adjusting the ratio of NH_3/He . The total flow rate of air in the air side was 50 ml/min. As shown in Fig. 4, selectivity of NO decreased slightly when increasing the concentration of ammonia, which could be due to favorable formation of N_2 under higher ammonia concentration as a result of the reaction of NH_x intermediates with NO formed and a recombination of adsorbed NH_x fragments [17]. In addition, It is can be detected that ammonia conversion is highest at lower flow rate (1.5 ml/min). The decrease of ammonia conversion as the flow rate of ammonia increases can be due to the lower contact time of ammonia with the catalytically active membrane surface. As shown in Fig. 4, it was observed that the oxygen permeation fluxes increased with the concentration of ammonia in the reactant. It is well known that, at a given temperature, the oxygen permeation

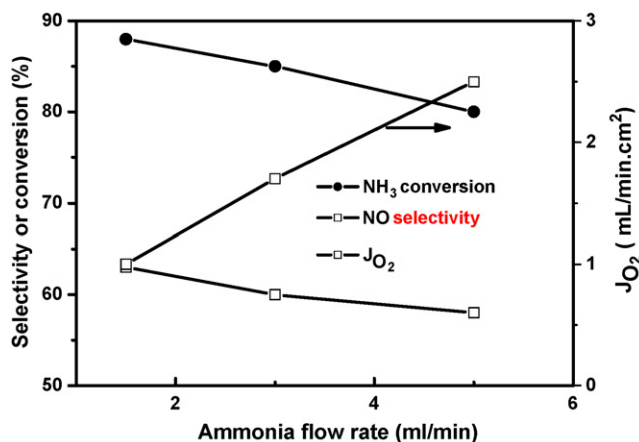


Fig. 4. Effect of ammonia flow rate on performance of membrane reactor at 800 °C. The total flow rate of the mixture of ammonia and He is 130 ml/min, air flow rate is 50 ml/min. Thickness of the membrane: 1.4 mm.

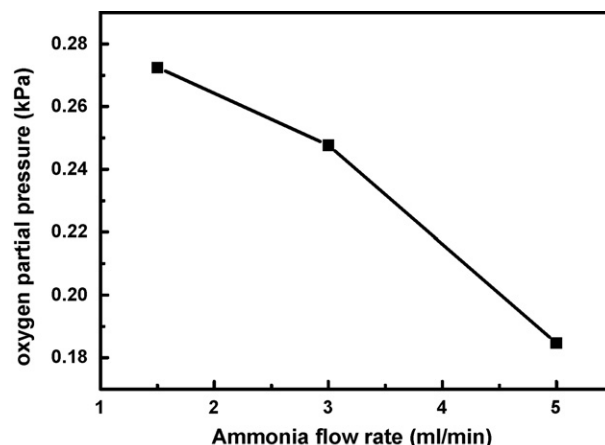


Fig. 5. Effect of ammonia flow rate on oxygen partial pressure of the reaction side at 800 °C. The total flow rate of the mixture of ammonia and He is 130 ml/min, air flow rate is 50 ml/min. Thickness of the membrane: 1.4 mm.

flux of the membrane is mainly determined by the oxygen gradient across the membrane. In the reaction side, more oxygen was needed to react with the ammonia when increasing the concentration of ammonia. As a result, the oxygen partial pressure near the membrane surface exposed to ammonia would decrease with increasing the ammonia flow rate (Fig. 5), which led to the increase of the oxygen permeation flux. This is consistent with previous reports that the oxygen flux strongly depends on the reactant flow rate [6,11].

3.3. Membrane stability in ammonia oxidation

The fresh and used $Ba_{0.5}Sr_{0.5}Co_{0.8}Fe_{0.2}O_{3-\delta}$ membranes were analyzed by SEM, EDS and XRD in an effort to understand the changes of the membrane during the reaction. Fig. 6 represents X-ray diffraction patterns of the fresh and used $Ba_{0.5}Sr_{0.5}Co_{0.8}Fe_{0.2}O_{3-\delta}$ membrane. For the fresh membrane sample, the XRD patterns showed a cubic perovskite structure with a lattice parameter of 3.9826 Å. However, most of the characteristic peaks of the perovskite phase of the used membrane weakened obviously. After reaction, the membrane surface exposed to NH_3 contained amount of BaO and CoO phase, which may be attributed to the decomposition of perovskite membrane. These results suggest that the perovskite structure in the reaction side was partially destroyed

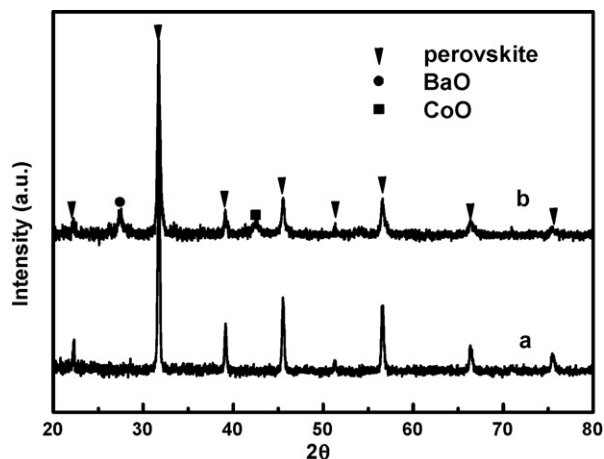


Fig. 6. X-ray diffraction patterns of: (a) fresh $Ba_{0.5}Sr_{0.5}Co_{0.8}Fe_{0.2}O_{3-\delta}$ membrane; (b) used $Ba_{0.5}Sr_{0.5}Co_{0.8}Fe_{0.2}O_{3-\delta}$ membrane surface exposed to NH_3 .

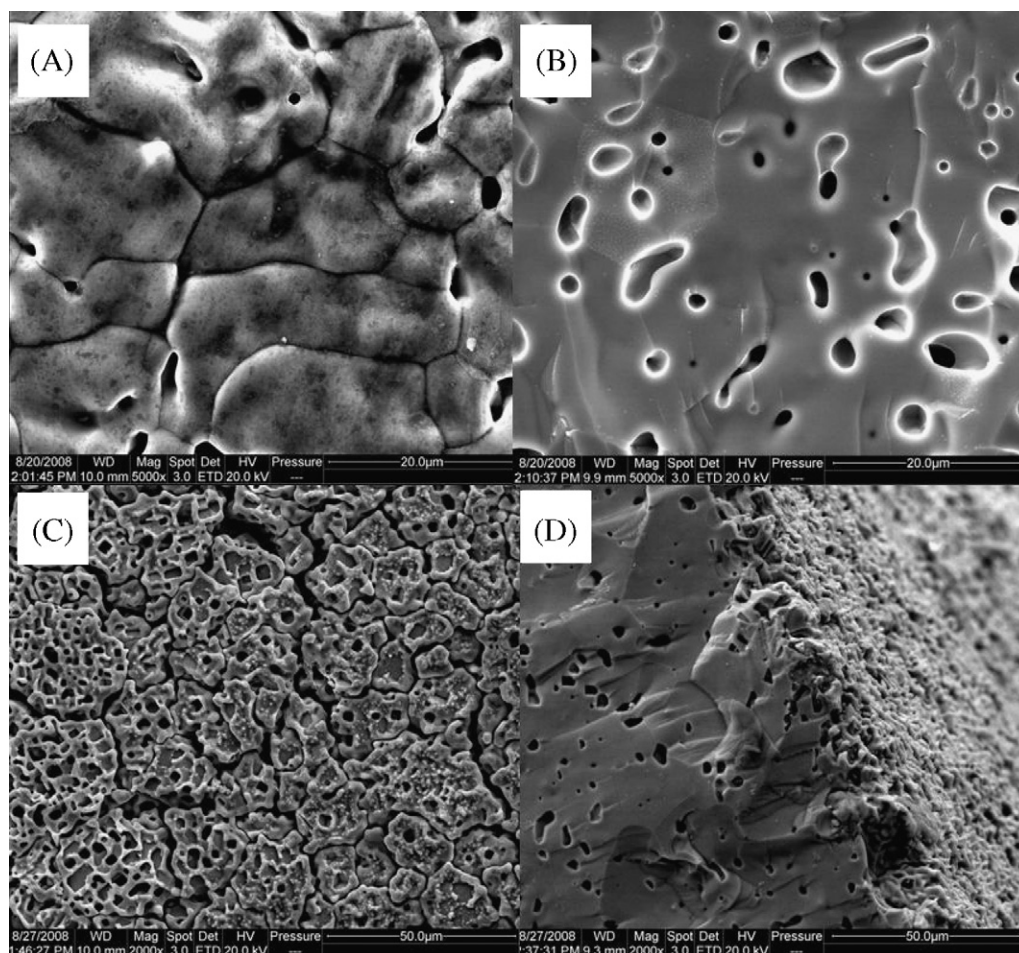


Fig. 7. SEM images of the fresh membrane and the used membrane. (A) and (B) were the surface and cross-section of fresh membrane, respectively; (C) was the surface of NH_3 side of the used membrane; (D) was the cross-section of near the NH_3 side.

during the reaction. Since NH_x species was produced in the reaction as intermediate and absorbed on the surface of the membrane, the reduction of the $\text{Ba}_{0.5}\text{Sr}_{0.5}\text{Co}_{0.8}\text{Fe}_{0.2}\text{O}_{3-\delta}$ would be unavoidable during the reaction. Fig. 7 shows the SEM images of the morphologies of fresh and used membrane. As shown in Fig. 7A, the fresh membrane exhibited significant clear grain boundaries. Though a few of pores can be found on the membrane surface, no open pores can be seen from the across-section of SEM image shown in Fig. 7B. Moreover, the oxygen permeation measurement confirmed that the open pores did not exist. The closed pores might be due to the grain growth or decomposition of the organic material during the sintering process [10]. For the used membrane, a porous layer appeared on the membrane surface exposed to NH_3 and the grain boundary is not visible shown in Fig. 7C, indicating that the membrane surface was decomposed in a strongly reducing and eroding atmosphere such as NH_3 and NO .

Table 1
EDS results of fresh membrane and used membrane.

Membrane	Section	Atomic %				
		Ba	Sr	Co	Fe	O
Fresh	Reaction side	10.5	11.3	16.9	4.3	57
	Middle	10.5	11.3	16.8	4.4	57
Used	Reaction side	9.6	15.1	20.9	6.9	47.5
	Middle	10.4	11.4	16.8	4.4	57

This development of the porous layer at the membrane surface after reaction were also observed by other researchers [18,19]. However, there was no obvious change for the membrane bulk as shown in Fig. 7D. The EDS analysis further confirmed the influence of reaction atmosphere on the membrane surface. Compared to the fresh membrane, it can be found from Table 1 that no composition changes of the cross-section can be detected for used membrane, suggesting that the membrane bulk is significant stable during the ammonia oxidation. While the obvious composition changes of the membrane surface on the reaction side can be observed for used membrane. Especially, the percentage of O decreased 10% compared to fresh membrane on the surface, which means BSCFO was reduced in the ammonia oxidation owing to the NH_x species produced in the reaction. These results are in good agreement with those of XRD. In addition, it can be detected that Fe and Co enriched on the surface after reaction. The segregation of transition metal cations on the membrane surface with reduction treatment has also been found by Wang et al. [13]. From above, it can be concluded that in order to develop a long-term membrane reactor for ammonia oxidation, the improvement of the stability of membrane needs to be carried out for further study.

4. Conclusion

Selective oxidation of ammonia to NO was studied in a dense mixed ion electron conducting $\text{Ba}_{0.5}\text{Sr}_{0.5}\text{Co}_{0.8}\text{Fe}_{0.2}\text{O}_{3-\delta}$ membrane

reactor. It is a new route for nitric acid production, in which pure oxygen can be in situ produced and N_2 in the air was totally removed in the reactor, especially, under reaction conditions, the environmental harmful N_2O was not detected and N_2 was the only N-containing by-product. Based on our results, it is concluded that the oxygen permeation flux through the dense membrane increases with increasing temperature and ammonia flow rate. Due to the weak oxygen bonding strength of $Ba_{0.5}Sr_{0.5}Co_{0.8}Fe_{0.2}O_{3-\delta}$, the lower reaction temperature favored the NO formation. And ammonia flow rate had considerable influence on NO selectivity, in which a decrease when increasing the concentration of ammonia was observed, because the reaction of NH_x intermediates with NO formed and a recombination of adsorbed NH_x fragments. Furthermore, it is found that the membrane surface exposed to the ammonia can be etched during the oxidation of ammonia, suggesting that the stability of the membrane must be improved.

Acknowledgements

This work was supported by the National Science Fund for Distinguished Young Scholars of China (Grant No. 20725313) and the Ministry of Science and Technology of China (Grant No. 2005CB221404).

References

- [1] E. Wagner, E. Fetzner, in: G. Ertl, H. Knözinger, J. Weitkamp (Eds.), *Handbook of Heterogeneous Catalysis*, VCH, Weinheim, 1997, pp. 1748–1761.
- [2] R.J. Farrauto, C.H. Bartholomew, *Fundamentals of Industrial Catalysis Process*, Chapman and Hall, Editors, London, 1997, p. 481.
- [3] V.I. Chernyshov, *Ammonia Combustion Plants (Review)*, NIITE Chim, Editor, Moscow, 1976, p. 70.
- [4] M.M. Karavayev, A.P. Zadorin, N.F. Kleshchev, *Catalytic Oxidation of Ammonia*, Khimia, Moscow, 1983.
- [5] N.F. Kleshchev, V.I. Atroshchenko, N.N. Nechiporenko, A.N. Butenko, N.P. Levshin, *Kataliz i Katalizatory* 14 (1976) 3.
- [6] J. Pérez-Ramírez, B. Vigeland, *Angew. Chem. Int. Ed.* 44 (2005) 1112.
- [7] J. Pérez-Ramírez, B. Vigeland, *Catal. Today* 105 (2005) 436.
- [8] Z.P. Shao, W.S. Yang, Y. Cong, H. Dong, J.H. Tong, G.X. Xiong, *J. Membr. Sci.* 172 (2000) 177.
- [9] H.H. Wang, Y. Cong, W.S. Yang, *Catal. Today* 104 (2005) 160.
- [10] H.H. Wang, Y. Cong, W.S. Yang, *Catal. Today* 82 (2003) 157.
- [11] H.H. Wang, Y. Cong, W.S. Yang, *J. Membr. Sci.* 209 (2002) 143.
- [12] H.H. Wang, C. Tablet, A. Feldhoff, J. Caro, *J. Membr. Sci.* 262 (2005) 20.
- [13] H.H. Wang, Y. Cong, W.S. Yang, *J. Membr. Sci.* 210 (2002) 259.
- [14] X.F. Chang, C. Zhang, Z.T. Wu, W.Q. Jin, N.P. Xu, *Ind. Eng. Chem. Res.* 45 (2006) 2824.
- [15] Y. Wu, T. Yu, B. Dou, C. Wang, X. Xie, Z. Yu, S. Fan, Z. Fan, L. Wang, *J. Catal.* 120 (1989) 88.
- [16] S.T. Liu, Z.L. Yu, Y. Wu, *Chin. J. Catal.* 52 (1994) 273.
- [17] V.A. Sadykov, L.A. Isupova, I.A. Zolotarevskii, L.N. Bobrova, A.S. Noskov, V.N. Parmon, E.A. Brushtein, T.V. Telyatnikova, V.I. Chernyshev, V.V. Lunin, *Appl. Catal. A* 204 (2000) 59.
- [18] H.J.M. Bouwmeester, *Catal. Today* 82 (2003) 141.
- [19] W.Q. Jin, S.G. Li, P. Huang, N.P. Xu, J. Shi, Y.S. Lin, *J. Membr. Sci.* 166 (2000) 13.